Electronic Supplementary Information (ESI)

Atomic Interpretation of High Activity on Transition Metal and Nitrogen Doped Carbon Nanofibers for Catalyzing Oxygen Reduction

Xingxu Yan,‡[ac] Kexi Liu,‡[b] Tuo Wang,[a] Yong You,[c] Jianguo Liu,[c] Peng Wang,[c] Xiaoqing Pan,[cd] Guofeng Wang,*[b] Jun Luo*[a] and Jing Zhu*[a]

[a.] National Center for Electron Microscopy in Beijing, School of Materials Science and Engineering, Key Laboratory of Advanced Materials (MOE) and The State Key Laboratory of New Ceramics and Fine Processing, Tsinghua University, Beijing 100084, China. *E-mail: luojunkink@126.com; jzhu@mail.tsinghua.edu.cn.

[b.] Department of Mechanical Engineering and Materials Science, University of Pittsburgh, Pittsburgh, PA 15261, USA. E-mail: guw8@pitt.edu.

[c.] National Laboratory of Solid State Microstructures, College of Engineering and Applied Sciences and Collaborative Innovation Center of Advanced Microstructures, Nanjing University, Nanjing 210093, China

[d.] Department of Chemical Engineering and Materials Science and Department of Physics and Astronomy, University of California - Irvine, Irvine, CA 92697, USA

‡ These authors contributed equally (X. X. Y. and K. X. L.).

1. TEM images and EDX spectra of catalysts.

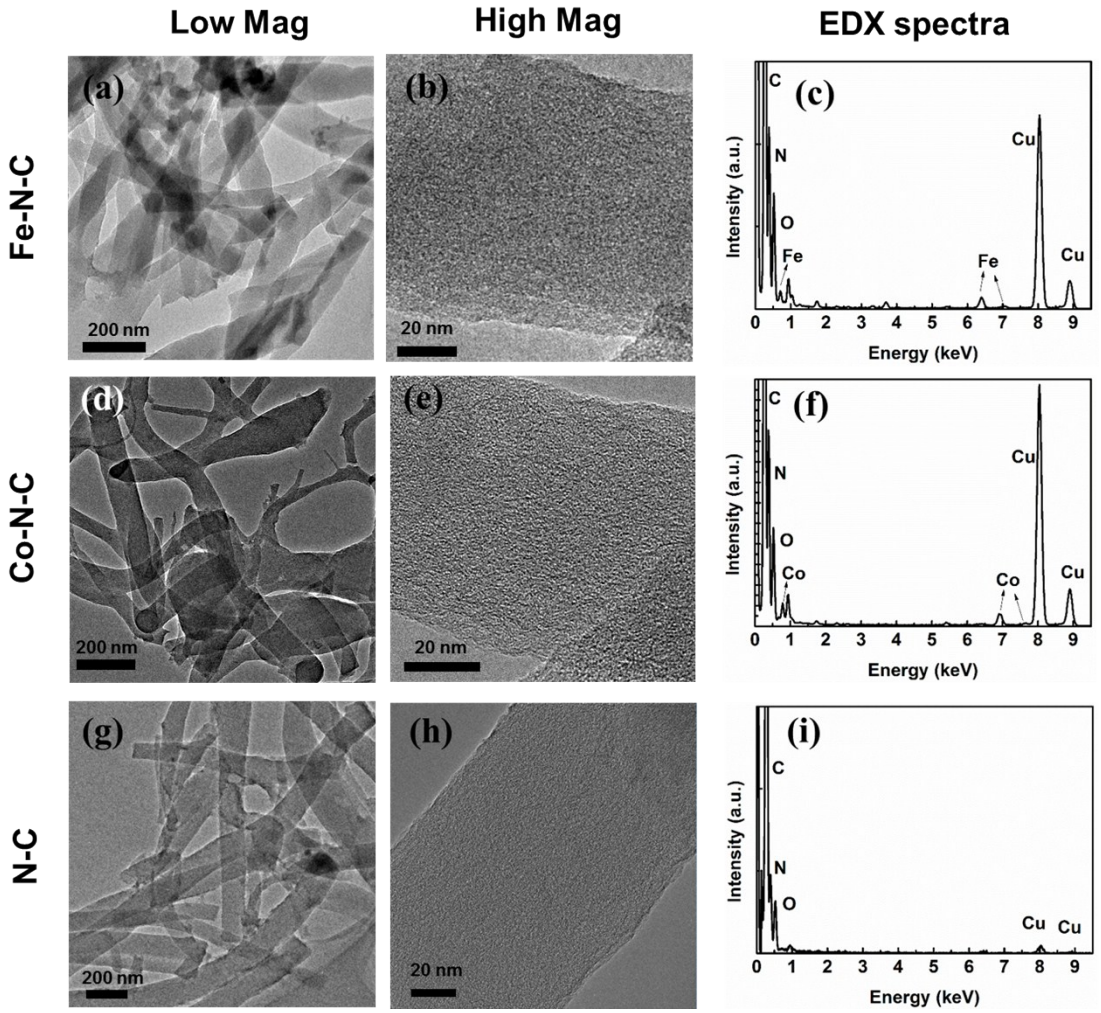

Fig. S1 Low (left panel) and high (middle panel) magnification transmission electron microscopy (TEM) images of Fe-N-C, Co-N-C and N-C catalysts, and corresponding EDX spectra (right panel), respectively. The signals of Cu are attributed to the copper grid.

2. Atomic contents from XPS results.

Table S1 Atomic contents of C, N, O and corresponding transition metal (TM) in Fe-N-C, Co-N-C and N-C catalysts.

Name	C (at. %)	N (at. %)	O (at. %)	TM (at. %)
Fe-N-C	79.19	14.84	5.7	0.28
Co-N-C	81.28	12.09	6.14	0.5
N-C	83.36	10.94	5.7	-

3. Atomic contents of nitrogen-containing groups.

Table S2 Atomic contents of pyridinic N, TM-N_x, pyrrolic N, quaternary N and pyridine oxide attained from the analysis of the XPS spectra of N 1s in Fig. 2d on Fe-N-C, Co-N-C and N-C catalysts.

Name	Pyridinic N (at. %)	TM-N_x (at. %)	Pyrrolic N (at. %)	Quaternary N (at. %)	Pyridine oxide (at. %)
Fe-N-C	4.57	2.24	2.35	2.07	3.61
Co-N-C	3.95	1.73	1.93	2.30	2.18
N-C	3.81	-	2.32	1.77	3.04

4. XPS spectra of various transition metals in TM-N-C catalysts.

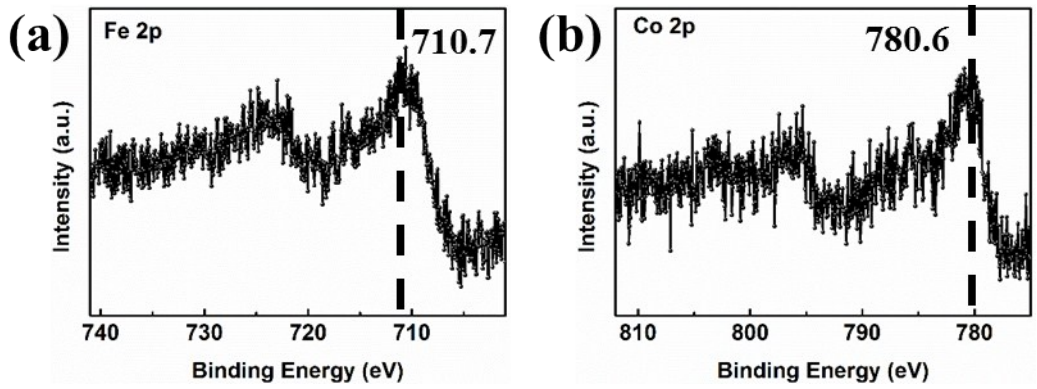

Fig. S2 XPS 2p spectra of (a) Fe and (b) Co in Fe-N-C and Co-N-C catalysts. The typical $2p_{3/2}$ binding energy of oxidized TM elements is found to be 710.7 eV (Fe, +3) and 780.0 eV (Co, +2). The experimental XPS data match with those binding energy of oxidized TM.

5. Comparison of catalytic activities.

Table S3 Catalytic activities of Fe-N-C, Co-N-C and N-C nanofiber catalysts, comparing with other published TM-N-C ones in acid and alkaline media. The reference number in the source column are same as those in the main text.

TM	Catalyst	$E_{1/2}$ [V versus RHE]		Source
		Acid	Alkaline	
Fe	Fe-N-C nanofibers	0.54	0.82	This work
	Polyaniline-Fe on carbon support	0.80	--	Ref. 8
	Fe-N-Doped Carbon Capsules	0.52	0.83	Ref. 11
	N-doped carbon nanotube and graphene complexes with iron	0.76	0.87	Ref. 18
	Pyridinic-Nitrogen-Dominated Graphene with Fe-N-C Coordination	--	0.84	Ref. 29
	Fe-porphyrin-like carbon nanotube	--	0.77	Ref. 60
Co	Co-N-C nanofibers	0.48	0.78	This work
	N-doped porous carbon materials with Co	--	0.80	Ref. 62
	Co_3O_4/N-doped graphene hybrid	--	0.83	Ref. 63
	Cobalt porphyrin-based conjugated mesoporous polymers	0.64	0.82	Ref. 64
	Polyaniline-Co on carbon support	0.77	--	Ref. 8
Metal -free	N-C nanofibers	0.34	0.72	This work
	Nitrogen-doped carbon nanocages	--	0.76	Ref. 61
	Nitrogen-doped multilayer graphene	--	0.75	Ref. 76
	Nitrogen-doped ultrathin carbon nanofibers	--	0.80	Ref. 12
	Polyaniline/polypyrrole on reduced graphene oxide	--	0.80	Ref. 23
	Nitrogen-doped graphene nanosheets	0.60	--	Ref. 79
	Ammonia-Treated Ordered Mesoporous Carbons	0.69	--	Ref. 14

6. Difference between half-wave potential in alkaline and acid media.

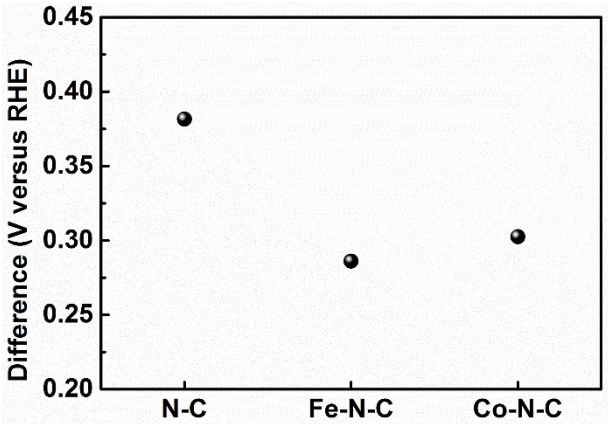

Fig. S3 Difference of half-wave potentials of Fe-N-C, Co-N-C and N-C catalysts for ORR in alkaline and acid media, calcuated from the corresponding data in Fig. 3b and 3d.

7. Lower magnification image of carbon nanofiber in Fe-N-C catalysts.

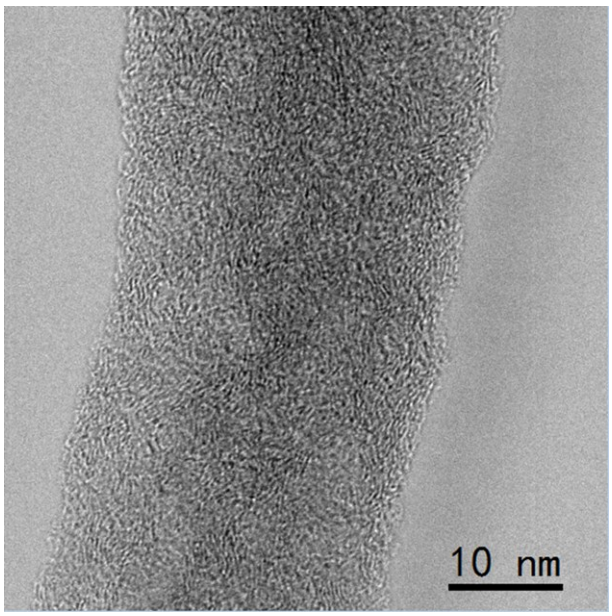

Fig. S4 Bright-Field (BF) STEM image of carbon nanofiber in Fe-N-C catalysts used in Fig. 4a and 4b of the manuscript. The diameter of carbon nanofiber is about 30 nm. The reason of choosing thinner nanofiber is to diminish the overlap of graphene-like nanoplates through the thickness direction on the edge side.

8. Associative Mechanism for ORR in acid and alkaline media.

It is worth mentioning that ORR proceeds differently in acid and in alkaline medium. In acid, the associative mechanism is

$$O_{2(aq)} + H^+ + e^- = OOH^*, \quad \text{(SR1a)}$$

$$OOH^* + H^+ + e^- = O^* + H_2O, \quad \text{(SR1b)}$$

$$O^* + H^+ + e^- = OH^*, \quad \text{(SR1c)}$$

$$OH^* + H^+ + e^- = H_2O, \quad \text{(SR1d)}$$

while in alkaline, the associative mechanism is

$$O_{2(aq)} + H_2O + e^- = OOH^* + OH^-, \quad \text{(SR2a)}$$

$$OOH^* + e^- = O^* + OH^-, \quad \text{(SR2b)}$$

$$O^* + H_2O + e^- = OH^* + OH^-, \quad \text{(SR2c)}$$

$$OH^* + e^- = OH^-, \quad \text{(SR2d)}$$

where the asterisk denotes the intermediates adsorbed on the active sites. The free energy of each ORR intermediates were calculated using the computational approach developed earlier by Nørskov et al. (*S1*) Specifically, the free energy of $H^+ + e^-$ at standard state can be indirectly calculated by the free energy of $\frac{1}{2}H_2$ in gas phase at standard state according to the definition of reversible hydrogen electrode,

$$G\left(\frac{1}{2}H_{2(g)}\right) = G(H^+) + G(e^-), pH = 0. \quad \text{(S1)}$$

Thus the free energy of ORR intermediates (OOH*, O* and OH*) in acid at pH = 0 can be calculated as

$$\Delta G_{ads} = G_{adsorbate-site} - G_{site} + xG(H_2) + (-e)U_{vs.\,RHE} - yG(H_2O) \quad \text{(S2)}$$

in which $G_{adsorbate-site}$ includes electronic energy and vibrational entropy; $G(H_2)$ is the free energy of H_2 in gas phase at standard state; $G(H_2O)$ is the free energy of H_2O in aqueous phase at standard state; e is the elementary charge; $U_{vs.\,RHE}$ is the electrode potential with respect to the reversible hydrogen electrode; *x* and *y* are the coefficient balancing the chemical equation. In alkaline, the free energy of ORR intermediates should be calculated in reference to OH^- which is the product of ORR. In order to compare the performance of the active sites in alkaline with that in acid, the state of reactants should be kept the same, using the equation

$$\Delta G_{ads} = G_{adsorbate-site} - G_{site} + x'G(H_2O) + (-e)U - y'G(OH^-), pH = 0 \quad \text{(S3)}$$

Due to ionization equilibrium of water, there is the following equation

$$G(H_2O) = G(H^+) + G(OH^-) \quad \text{(S4)}$$

Replacing $G(OH^-)$ with $G(H_2O) - G(H^+)$ in equation S3, we can get equation S2. Therefore, the free energy landscapes of ORR look the same thermodynamically no matter in acid or in alkaline. In present study, we calculated the free energy diagram using equation S2 both in acid and alkaline.

9. Electron Transfer Number.

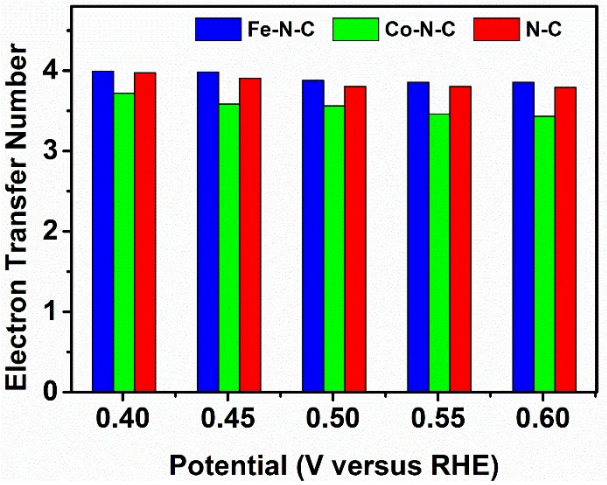

Fig. S5 Number of electrons transferred during the ORR on Fe-N-C, Co-N-C and N-C catalysts in oxygen-saturated 0.1 mol/L KOH solution. The data were acquired by varying rotation speed at 400, 625, 900, 1225, 1600 and 2025 rpm and calculated by using Koutecky-Levich equation.(*S2*) The average values of electron transfer number on Fe-N-C, Co-N-C and N-C catalysts are 3.91, 3.55 and 3.86 at the voltage range from 0.4 to 0.6 V versus RHE, respectively.

REFERENCES

S1. J. K. Nørskov, J. Rossmeisl, A. Logadottir, L. Lindqvist, J. R. Kitchin, T. Bligaard and H. Jónsson, *J. Phys. Chem. B*, 2004, **108**, 17886-17892.

S2. A. J. Bard and L. R. Faulkner, *Electrochemical Methods: Fundamentals and Applications*, 2nd ed.; Wiley: New York, 2001.